JOURNAL OF GUIDANCE, CONTROL, AND DYNAMICS
Vol. 28, No. 2, March–April 2005

Simple Strategy for Geostationary Stationkeeping Maneuvers Using Solar Sail

Christian Circi*
University of Rome "La Sapienza," 00184 Rome, Italy

This study deals with solar-sail applications to geostationary satellites and the analysis of stationkeeping maneuvers. A thrust strategy for north–south maneuvers is found as a function of the lunar inclination and the solar-sail's characteristic acceleration. The characteristic acceleration obtained for north–south maneuvers is used for the east–west maneuvers thrust strategy. The dependence with respect to the Earth's position around the sun and the sun-Earth-spacecraft relative position are analyzed for both types of maneuvers. The solar-sail stationkeeping performances are presented as a function of the geostationary satellite longitude, and the results are given for a one-year simulation. A comparison with chemical propulsion systems, from the total mass point of view, is presented. The reorbiting maneuver at the end of the operational life is also considered, and the extra propellant necessary for a chemical engine is evaluated.

Introduction

WITH a solar sail, no propellant mass is necessary, and high performances using this technology are expected for the future.[1] Several kinds of missions with solar sail as a propulsion systems have been proposed: Salvail and Stuiver[2] investigate the problem of transfer to the moon from a geosynchronous orbit; Leipold et al.[3] study the mission for a Mercury polar orbiter, and McInnes et al.[4] have presented an investigation of the use of solar-sail propulsion for both Mercury orbiter and Mercury sample return missions. Jayaraman[5] and Otten and McInnes[6] present optimum trajectories for Mars missions. High-performance solar sails suggest nonclassical missions: Powers and Coverstone[7] analyze the transfer to Earth and Mars synchronous orbits; McInnes[8,9] to the lunar L_2 Lagrange point and to "levitation" orbits, where the solar radiation pressure acceleration balances solar gravity, while rendezvous missions with asteroids is studied by Morrow et al.[10] The solar radiation pressure has also been proposed for attitude control: for a geostationary satellite by Modi and Kumar,[11] for a satellite in an elliptic orbit by Joshi and Kumar,[12] and for an interplanetary spacecraft by Sirinian.[13] Neglecting the effects of gravitational attraction of the moon, the sun, and the terms in the Earth's gravity potential function of order larger than two, the use of a solar sail for east–west stationkeeping maneuvers for geosynchronous satellites is proposed by Black et al.[14] Black uses a very small solar sail and a simple thrust strategy, but the results are unusable for geostationary satellite deadband requirements. In this paper solar radiation pressure is used as a propulsive force for both east–west and north–south stationkeeping maneuvers for a geostationary satellite, usually made by a chemical engine.[15] At the Earth's distance from the sun, the solar pressure is strong enough to perform stationkeeping with the solar sail. Even if only a small acceleration is available, the thrust can be applied for long period because no propellant mass is required by the sail. However, geometrical constraints, caused by the relative sun-Earth-satellite position, must be considered.

Stationkeeping Maneuvers

The ground track of geostationary satellites is constrained to remain within a rectangular box containing the ground station. The satellite is forced away from the box by the harmonics of the Earth's gravity field (J_2, J_{22}, ...), the luni–solar effect and solar radiation pressure. The longitude deadband is usually expressed in the form $\lambda_m \pm \delta\lambda$, where λ_m is the nominal longitude and $\delta\lambda$ the maximum drift longitude (Fig. 1). The box side depends on the mission requirements, but a typical range for $\delta\lambda$ and the maximum inclination $i_{\max}$, is from 0.1 to 0.5 deg. Stationkeeping maneuvers are generally classified as north–south to reduce the inclination i and consequently the satellite elevation with respect to the equatorial plane, and as east–west, to control the satellite longitude.

An inertial *X, Y, Z* reference frame and a local r, ϑ, h reference frame (radial, transverse, and normal direction, respectively) are considered in the simulation (Fig. 2). The solar-radiation-pressure (SRP) forces are as a result of photons impinging on the sail surface. A fraction of the impinging photons are adsorbed ρ_a, a fraction are specularly reflected ρ_s, and a fraction are diffusely reflected by a surface ρ_d, so that we have $\rho_a + \rho_s + \rho_d = 1$. The SRP force acting on a flat surface located at one astronomical unit from the sun can be modeled as[16]

$$\boldsymbol{F} = PA(\boldsymbol{S}\cdot\boldsymbol{n})\left\{(1-\rho_s)\boldsymbol{S} + \left[2\rho_s(\boldsymbol{S}\cdot\boldsymbol{n}) + \tfrac{2}{3}\rho_d\right]\boldsymbol{n}\right\} \qquad (1)$$

where $P = 4.563 \times 10^{-6}\ N/M^2$ is the solar radiation pressure at one astronomical unit from the sun, A is the sail surface area, $\boldsymbol{n}$ is a unit vector normal to the sail surface, and $\boldsymbol{S}$ is a unit vector pointing from the sun to the surface. The SRP force acting on a sail surface with an area A is often approximated as[16]

$$F \approx \eta PA\cos^2\alpha \qquad (2)$$

where α is the angle between the sun-sail line and the sail normal, and η is the overall sail thrust coefficient, typically around 1.8 for a real sailcraft with sail wrinkles and billowing, with an ideal maximum value of $\eta_{\max} = 2$. The following assumptions are considered: 1) flat solar sail, 2) thrust direction along only the sail normal on the dark side, and 3) thrust coefficient $\eta = 1.8$. In the local r, ϑ, h reference frame two angles defined the orientation of the sail normal vector $\boldsymbol{n}$ and so the thrust direction. The antenna points towards the earth on $-r$ direction, while the sailcraft is steered changing the center-of-mass location with respect to the center-of-pressure location. This can be achieved employing reflective control vane mounted at the spar tips.[16] However, different solar-sail architecture are been suggested for this purpose.[16,†]

Received 1 December 2003; revision received 19 May 2004; accepted for publication 8 June 2004.

*Assistant Professor, Department of Aerospace and Astronautical Engineering, Scuola di Ingegneria Aerospaziale, v. Eudossiana 16; christian.circi@uniromal.it.

†Data available online at http://www.planetary.org/solarsail/ss_spacecraft/index.html [cited 18 March 2004].

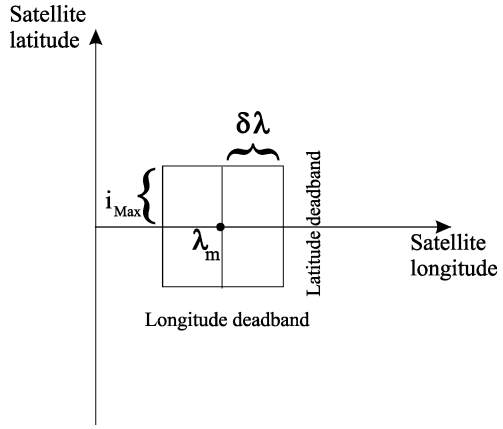

Fig. 1 Typical deadband for stationkeeping maneuvers.

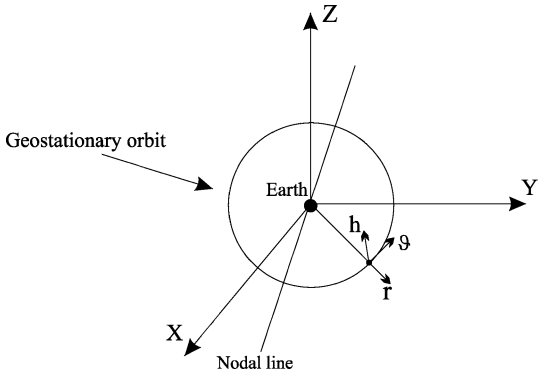

Fig. 2 Reference frames considered.

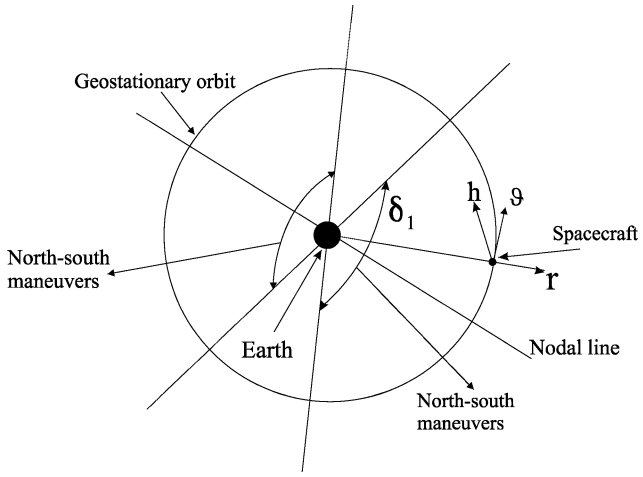

Fig. 3 North–south stationkeeping maneuvers regions.

North–South Stationkeeping Maneuvers

The solar and lunar gravitational forces, together with the precession caused by J_2, change the satellite inclination and play a key role in the out-of-plane motion. The total mean drift rate varies between 0.75 and 0.95 deg/year, depending on the value of the moon's inclination with respect to the Earth's equatorial plane. The moon's inclination changes, over a 18.6-year period, from 18.3 to 28.58 deg and consequently also the stationkeeping ΔV (Ref. 15).

If the solar sail is used as a propulsive system, the sun-Earth-satellite relative position must be taken into account. The north–south maneuvers are centered around the nodal line (intersection of the Earth's equatorial plane and the satellite's orbital plane), by an angle with an amplitude of δ_1 (Fig. 3). The high-efficiency thrust direction is perpendicular to the orbital plane, during the descending node in the h direction and during the ascending node in the $-h$ direction. But sometimes the solar sail is not able to provide thrust parallel to one axis because this depends on the sunlight direction. For this reason, a steering law that maximizes the force component along the h direction f_h, with respect to the total modulus $f_{\text{Tot}} = \sqrt{(f_r^2 + f_\vartheta^2 + f_h^2)}$ is used for the descending node case f_h/f_{Tot}, while for the ascending node case the steering maximizes $-f_h/f_{\text{Tot}}$. The amplitude of the angle δ_1 is directly related to the sail area. By increasing δ_1, the north–south maneuvers are applied for more time, and the sail surface area can be reduced. Numerical simulation shows that with δ_1 bigger than 140 deg the maneuver's efficiency decreases and the sail produces only a negligible variation in inclination. For this reason the amplitude of the angle δ_1 is set at 140 deg. During the Earth's orbit around the sun, the north–south maneuver is not made around the equinoctial line for an angle with an amplitude of δ_2 (Fig. 4). In this region, in fact, because of the relative sun-Earth-spacecraft position, the sail will not be able to eliminate, or reduce enough, the radial thrust component f_r, present in the f_{Tot} term. This component reduces the steering efficiency and must be eliminated for inclination change maneuvers. Numerical simulations show that this component cannot be eliminated, or reduced enough, for angles centered with respect to the equinoctial line less than 40 deg. For this reason, the amplitude of δ_2 angle is set at 40 deg. When the Earth is in this region, for about 40 days, the satellite's inclination increases (to Δi). After this period the solar sail must be able to reduce the inclination to zero before the beginning of the next region where the north–south maneuver is not made.

Figure 5 shows the maximum value for the geostationary satellite inclination, obtained using the previous steering law for a one-year simulation, as a function of the solar-sail characteristic acceleration

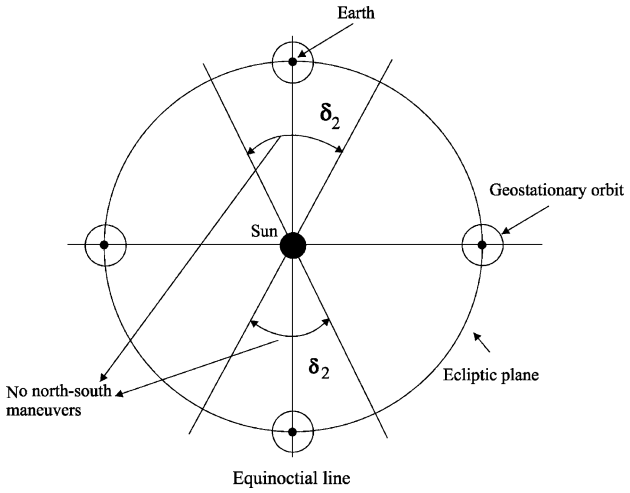

Fig. 4 Regions where the north–south maneuvers are not made.

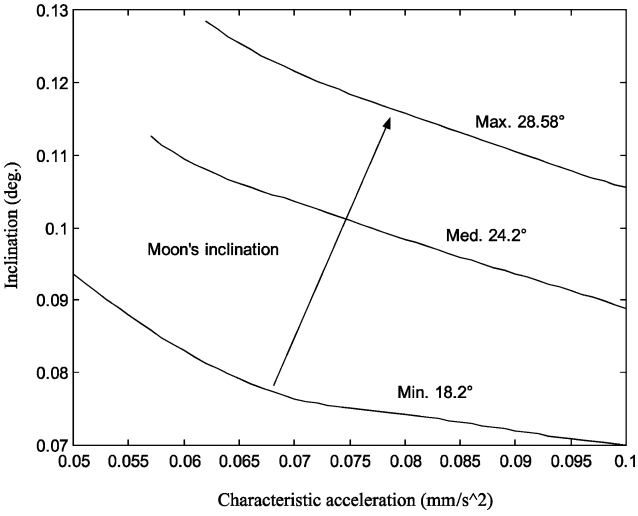

Fig. 5 Solar-sail performance to control the geostationary satellite inclination.

a_c and the lunar inclination. In the simulation, the solar and the lunar gravitational forces and the first four tesseral and zonal harmonics of the Earth's gravity field are considered. The figure shows the comparison between three different cases: when the moon's inclination is at its maximum, medium, and minimum values with respect to the Earth's equatorial plane. With the same a_c, the smallest inclination is obtained when the moon's inclination is at its minimum. The end of the curve, on the left side, indicates the smallest a_c value able to reduce the inclination to zero. For a_c less than this value, the inclination at the beginning of the next region, where the north–south maneuvers are not made, is not zero but Δi. This fact makes the geostationary satellite increase its inclination by $2\Delta i$ every year, and ground-track control is impossible. To design a 10-year lifetime geostationary satellite, with the minimum ΔV required for the north–south maneuvers, it is necessary to select the initial date when the moon's inclination is 24.2 deg in descending direction. In this case the moon's inclination assumes the same value (24.2 deg) only after 10 years. The out-of-plane perturbations are at a maximum when the moon's inclination is maximum, and this happens at the beginning and at the end of this period. In Fig. 5 the intermediate line corresponds to the simulation when the moon's inclination is equal to 24.2 deg, and the satellite's inclination remains under 0.11 deg if $a_c = 0.057$ mm/s^2 is used. This value of a_c is now used for east–west maneuvers.

East–West Stationkeeping Maneuvers

Longitude stationkeeping needs less fuel than inclination stationkeeping but is more complex. A tangential burn does not change the satellite longitude directly, but only its time derivative. A tangential burn also changes the orbital eccentricity, which influences the longitude librations. The longitude control is still more complicated if low-thrust propulsion systems are used. In fact, in this case also the longitude derivative does not change directly, but depends on the duration of the thrust. If a solar sail is used, constraints on the thrust direction and the thrust magnitude with respect to the sail attitude must be added.

To control the longitude, the thrust is applied for an angle with amplitude $2\delta_3$ centered with respect to the perpendicular of the nodal line (Fig. 6). The different geometrical positions with respect to the sun during the year suggest the division of the thrust strategy maneuvers into four quadrants (Fig. 7). Each quadrant is centered with respect to the equinoctial line or with respect to the solstice line. During the quadrants centered with respect to the equinoctial line, the strategy maximizes the tangential component $\pm f_\vartheta$: inside these quadrants the sunlight direction allows a large reduction of the radial and vertical thrust components f_r, f_h. During the quadrants centered with respect to the solstice line, the thrust strategy maximizes the tangential component with respect to the total thrust modulus $\pm f_\vartheta / f_{\mathrm{Tot}}$. In this case the radial and normal thrust components cannot be eliminated, and this strategy makes a good compromise between the necessity to increase the tangential component and to reduce the other. The sign + or − depends on the actual value of ground track $\delta\lambda$ with respect to the reference longitude (Fig. 8). If $\delta\lambda > 0$, the sign + is selected. In fact, a positive tangential force

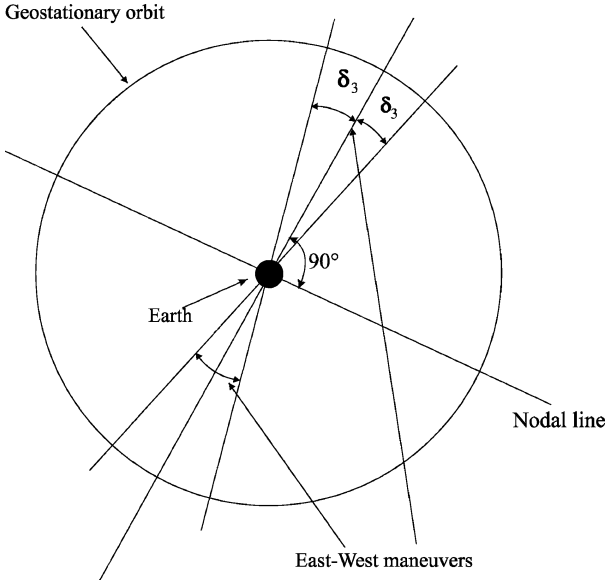

Fig. 6 Region where the thrust strategy for east–west maneuvers is applied.

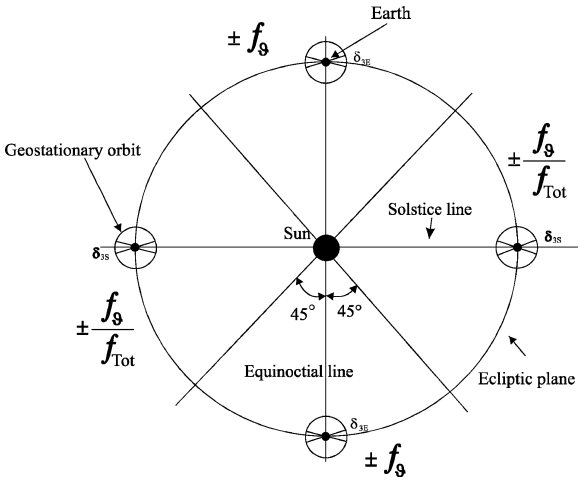

Fig. 7 Quadrants for east–west maneuvers thrust strategy.

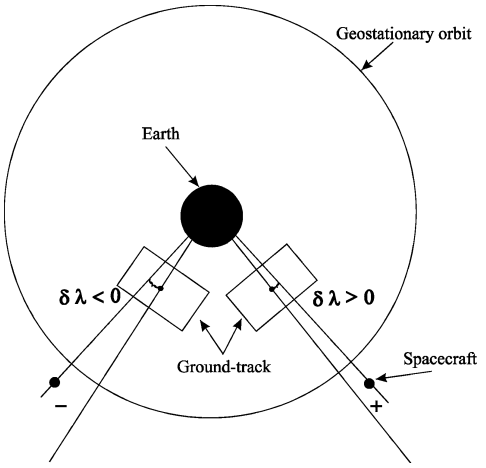

Fig. 8 Definition of the sign for the steering during the east–west maneuvers.

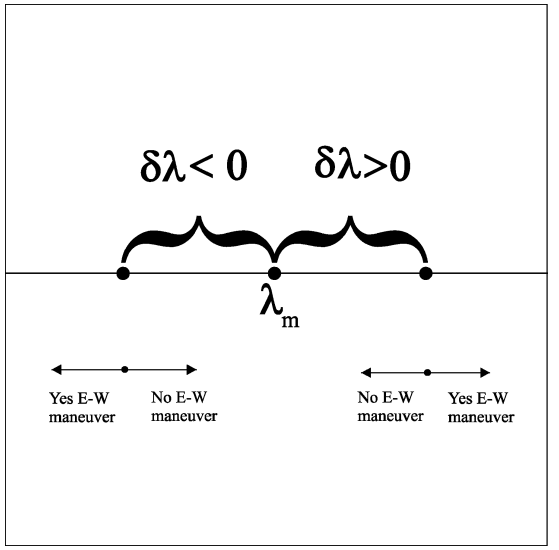

Fig. 9 Case in which east–west maneuvers are applied or not.

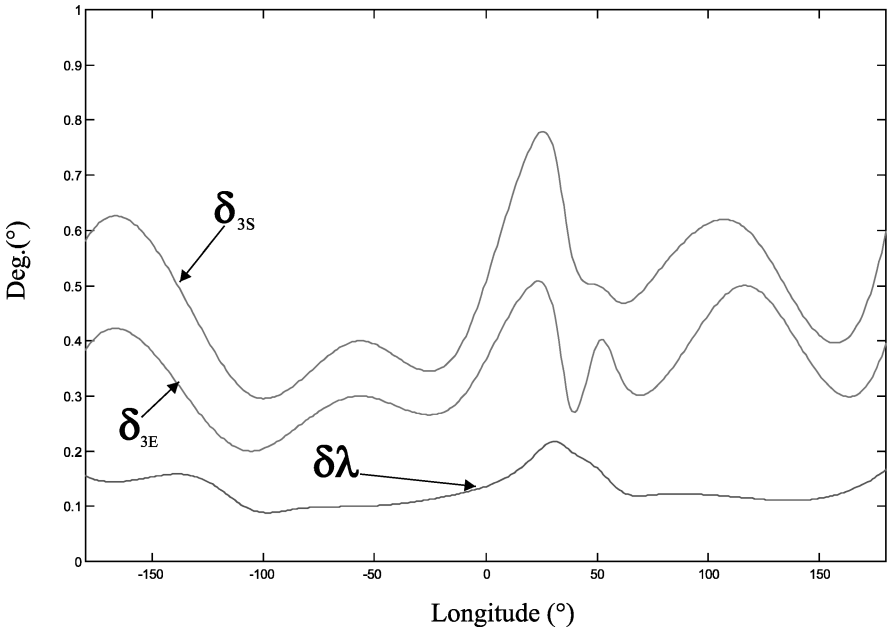

Fig. 10 Values for $\delta\lambda$, δ_{3E}, δ_{3S} as a function of geostationary satellite longitude.

Table 1 Ten-year stationkeeping maneuver performance

	Satellite mass, kg				
Parameter	1500	1000	500	350	300
Chemical propulsion, kg	300	216.7	133.3	108.3	100.0
Sail mass, kg	100	65.6	32.5	23	19.3
Square sail side, m	100	81	57	48	44

increases the semimajor axis and the orbital period, reducing $\delta\lambda$. If $\delta\lambda < 0$, the $-$ sign is used. In fact, a negative tangential force reduces the orbital period, the spacecraft increases its velocity, and $\delta\lambda$ decreases.

Because of the different geometrical conditions, the amplitude of the δ_3 angle is not the same in different quadrants: in particular, in equinoctial quadrants, it is indicated by δ_{3E}, whereas for solstice quadrants δ_{3S} (Fig. 7). The values for δ_{3E} and δ_{3S} angles are obtained with a parametric search to reduce $\delta\lambda$.

Finally, the east–west maneuvers are used only if the satellite ground track increases the distance from the nominal longitude; otherwise, no thrust is applied. For example, if $\delta\lambda$ is positive but the satellite ground track goes towards the nominal longitude, no thrust strategy is applied (Fig. 9).

Results

The thrust strategy described in preceding sections is applied to control the ground track of a geostationary satellite. In the simulation, the solar and the lunar gravitational forces and the first four tesseral and zonal harmonics of the Earth's gravity field are considered. Figure 10 shows the $\delta\lambda$ obtained for each longitude value for a one-year simulation. The $\delta\lambda$ is not always the same and varies from 0.09 to 0.21 deg as a function of the reference longitude. Also the angles δ_{3E} and δ_{3S} change with the longitude, and the values in Fig. 10 are obtained with a parametric search to reduce $\delta\lambda$. To analyze the performances from the mass point of view, the mass necessary using a chemical engine (with specific impulse $I_{sp} = 280$ s and 50 kg of engine dry mass) is compared with the solar-sail mass. An assembly loading of 10 gm^{-2} comprising the coated sail film, deployable booms, and control mechanisms is supposed.[4] There is intense research activity to develop new technology and structural optimization software to decrease the solar-sail mass.[17,18]

Table 1 shows the geostationary stationkeeping maneuver performances, for a 10-year lifetime satellite, as a function of satellite mass and propulsion system. The propellant mass calculation for a chemical engine is based on the typical ΔV required by a geostationary satellite, variable from 42 to 52 m/s per year and tabulated on.[15] Solar-sail performances are very advantageous with respect to the classical chemical engine and increase when the total satellite mass is reduced. The solar-sail dimension depends on the satellite mass and characteristic acceleration. For a square solar sail the last line in Table 1 shows the sail side as a function of the satellite mass for $a_c = 0.057$ mm/s^2.

Another opportunity to save propellant is given at the end of the mission when the geostationary satellite is put into a graveyard orbit (geostationary altitude +250 km). This maneuver, for a 1500-kg satellite, requires about 5 kg of propellant using a chemical engine, whereas using solar sail this phase is made without additional propellant.

Conclusions

The use of solar sail for north–south and east–west stationkeeping maneuvers for a geostationary satellite has been proposed. The minimum characteristic acceleration for north–south maneuvers is found as a function of the moon's inclination and the amplitude required for the ground-track deadband. For a 10-year lifetime a characteristic acceleration of 0.057 mm/s^2 is enough to force the inclination under 0.11 deg. This characteristic acceleration value is used for east–west maneuvers and the proposed thrust strategy is able to control the satellite ground track in a small rectangular box with the maximum drift longitude from 0.09 to 0.21 deg, depending on the nominal longitude value. A comparison with respect to a chemical propulsion system is presented as a function of the total satellite mass. The benefit of using a solar sail increases when the total satellite mass is reduced, and for a 300-kg satellite the side for a square solar sail is only 44 m.

Acknowledgments

The author gratefully acknowledge F. Graziani, P. Teofilatto, and S. Sgubini for their comments and suggestions.

References

[1]Leipold, M., Kassing, D., Eiden, M., and Herbeck, L., "Solar Sails for Space Exploration—The Development and Demonstration of Critical Technologies in Partnership," *ESA Bulletin*, No. 98, June 1999, pp. 102–107.

[2]Salvail, J. R., and Stuiver, W., "Solar Sailcraft Motion in Sun–Earth–Moon Space with Application to Lunar Transfer from Geosynchronous Orbit," *Acta Astronautica*, Vol. 35, No. 2–3, 1995, pp. 215–229.

[3]Leipold, M., Seboldt, W., Lingner, S., Borg, E., Herrmann, A., Pabsch, A., Wagner, O., and Bruckene, J., "Mercury Sun-Synchronous Polar Orbiter with a Solar Sail," *Acta Astronautica*, Vol. 39, No. 1–4, 1996, pp. 143–151.

[4]McInnes, C. R., Hughes, G., and McDonald, M., "Low Cost Mercury Orbiter and Sample Return Missions Using Solar Sail Propulsion," *Aeronautical Journal*, Vol. 107, Aug. 2003, pp. 469–478.

[5]Jayaraman, T. S., "Time-Optimal Orbit Transfer Trajectory for Solar Sail Spacecraft," *Journal of Guidance and Control*, Vol. 3, No. 6, 1980, pp. 536–542.

[6]Otten, M., and McInnes, C. R., "Near Minimum-Time Trajectories for Solar Sails," *Journal of Guidance, Control, and Dynamics*, Vol. 24, No. 3, 2001, pp. 632–634.

[7]Powers, R. B., and Coverstone, V. L., "Optimal Solar Sail Orbit Transfers to Synchronous Orbits," *Journal of the Astronautical Sciences*, Vol. 49, No. 2, 2001, pp. 269–281.

[8]McInnes, C. R., "Solar Sail Trajectories at the Lunar L_2 Lagrange Point," *Journal of Spacecraft and Rockets*, Vol. 30, No. 6, 1993, pp. 782–784.

[9]McInnes, C. R., "Inverse Solar Sail Trajectory Problem," *Journal of Guidance, Control, and Dynamics*, Vol. 26, No. 2, 2003, pp. 369–371.

[10]Morrow, E., Scheeres, D. J., and Lubin, D., "Solar Sail Orbit Operations at Asteroids," *Journal of Spacecraft and Rockets*, Vol. 38, No. 2, 2001, pp. 279–286.

[11]Modi, V. J., and Kumar, K., "Attitude Control of Satellite Using the Solar Radiation Pressure," *Journal of Spacecraft and Rockets*, Vol. 9, No. 9, 1972, pp. 711–713.

[12]Joshi, V. K., and Kumar, K., "New Solar Attitude Control Approach for Satellites in Elliptic Orbits," *Journal of Guidance and Control*, Vol. 3, No. 1, 1980, pp. 42–47.

[13]Sirinian, M., "Sulla Possibilità di Realizzare una Sonda Solare Semplice Stabilizzata Mediante la Pressione d'Irraggiamento," *Atti del Centro Ricerche Aerospaziali*, No. 40, March 1974, pp. 1–30 (in Italian).

[14]Black, W. L., Crocker, M. C., and Swenson, E. H., "Stationkeeping a 24-Hr Satellite Using Solar Radiation Pressure," *Journal of Spacecraft and Rockets*, Vol. 5, No. 3, 1968, pp. 335–337.

[15]Soop, E. M., "Introduction to Geostationary Orbits," European Space Operations Centre, Orbit Attitude Divi., ESA SP-1053, Darmstadt, Germany, Nov. 1983.

[16]Wie, B., "Dynamics Modeling and Attitude Control of Solar Sail Spacecraft," NASA, JPL Contract No. 1228156, Final Rept., 10 Jan. 2002.

[17]Greschik, G., and Mikulas, M. M., "Design Study of a Square Solar Sail Architecture," *Journal of Spacecraft and Rockets*, Vol. 39, No. 5, 2002, pp. 653–661.

[18]Murphy, D. M., Murphey, T. W., and Gierow, P. A., "Scalable Solar Sail Subsystem Design Concept," *Journal of Spacecraft and Rockets*, Vol. 40, No. 4, 2003, pp. 539–547.